文章编号: 1000-324X(2022)03-0289-08 **DOI:** 10.15541/jim20210518

橙黄光玻璃陶瓷的光固化成型与无压烧结

李 琪[1], 黄 羿[1], 钱 滨[2], 许贝贝[1], 陈莉英[1], 肖文戈[1], 邱建荣[1]

(1. 浙江大学 光电科学与工程学院, 杭州 310027; 2. 宁波匠心快速成型技术有限公司, 宁波 315000)

摘 要: 传统“荧光粉+有机硅脂”荧光转换体的热导率低, 且物理化学稳定性差, 不能应用于高功率白光 LED 领域。全无机荧光块体材料可以规避有机封装, 具有更高的热导率, 但这类材料面临着成本高且极难实现立体结构的问题。本工作基于非晶态纳米二氧化硅, 得到一种包含(Gd,Y)AG:Ce 荧光粉、可在紫外光下固化的浆料, 并通过光固化成型、空气排脂、无压烧结, 制备了一种(Gd,Y)AG:Ce 荧光粉–石英玻璃复合材料。该荧光玻璃陶瓷在蓝光激发下发射峰值位于 575 nm 的宽带橙黄光, 且内量子效率大于 90%。研究结果表明, 在致密化烧结过程中, (Gd,Y)AG:Ce 荧光粉与石英玻璃之间的界面反应非常微弱, 因此荧光粉能够完好地嵌入到石英玻璃中。该全无机荧光转换体可以用于封装相关色温小于 4500 K、显色指数大于 75 和流明效率为 74 lm·W^{-1} 的高功率暖白光 LED。所构建的激光照明器件的饱和激光功率密度可达 2.84 W·mm^{-2}, 此时光通量为 180 lm。此外, 所提出的制备方法与 3D 打印兼容, 可以批量化制造出具有复杂立体结构的荧光转换体。该技术有望推动高功率白光 LED 朝着个性化和模块化发展。

关 键 词: 荧光粉; 玻璃陶瓷; 暖白光; 3D 打印

中图分类号: TQ174 **文献标志码:** A

Photo Curing and Pressureless Sintering of Orange-emitting Glass-ceramics

LI Qi[1], HUANG Yi[1], QIAN Bin[2], XU Beibei[1], CHEN Liying[1], XIAO Wenge[1], QIU Jianrong[1]

(1. School of Optical Science and Engineering, Zhejiang University, Hangzhou 310027, China; 2. Ningbo Ingenuity Rapid Prototyping Technology Co., Ltd., Ningbo 315000, China)

Abstract: Because of low thermal conductivity and weak physical and chemical stabilities, traditional “phosphor in silicone” color converters are precluded from high-power white LED applications. All-inorganic bulk luminescence materials not only can circumvent organic encapsulation, but also have higher thermal conductivity. However, those bulk materials are high in cost and very difficult to be shaped into three-dimensional structures. Here, based on amorphous silica nanoparticles, a slurry, containing (Gd,Y)AG:Ce phosphor powders and can be polymerized under UV light, were developed. Bulk (Gd,Y)AG:Ce-silica glass composites were prepared successfully through photo curing, debinding in air and pressureless sintering. Under excitation of blue light, these luminescence glass-ceramics exhibit broadband orange emission peaking at 575 nm with internal quantum efficiency higher than 90%. Our results show that the interfacial reaction between (Gd,Y)AG:Ce and silica glass is very weak, and thus the former

收稿日期: 2021-08-23; **收到修改稿日期:** 2021-09-24; **网络出版日期:** 2021-11-01

基金项目: 浙江省重点研发计划(2021C01024); 中国博士后科学基金(2021M692840); 浙江大学现代光学仪器国家重点实验室开放基金
Provincial Key R&D Program of Zhejiang (2021C01024); China Postdoctoral Science Foundation (2021M692840); Open Fund of the State Key Laboratory of Modern Optical Instrumentation, Zhejiang University

作者简介: 李 琪(1998–), 女, 硕士研究生. E-mail: 22030030@zju.edu.cn
LI Qi (1998–), female, Master candidate. E-mail: 22030030@zju.edu.cn

通信作者: 肖文戈, 助理研究员. E-mail: wengsee@zju.edu.cn; 邱建荣, 教授. E-mail: qjr@zju.edu.cn
XIAO Wenge, lecturer. E-mail: wengsee@zju.edu.cn; QIU Jianrong, professor. E-mail: qjr@zju.edu.cn

can be well embedded into bulk silica glass. Such all-inorganic color converters were further used to fabricate high-power warm white LEDs with correlated color temperature smaller than 4500 K, color rendering index higher than 75, and luminous efficiency of 74 $lm \cdot W^{-1}$. Luminescence saturation threshold of the as-fabricated laser lighting device is as high as 2.84 $W \cdot mm^{-2}$, where its luminous flux can achieve 180 lm. Moreover, preparation of (Gd,Y)AG:Ce-silica glass composites is compatible to 3D printing technology, thus allowing the mass manufacturing of color converters with complex 3D structures, which may promote personalization and modularization of high-power white LEDs.

Key words: phosphors; glass-ceramics; warm white light; 3D printing

半导体发光二极管(Light emitting diodes, LED)因体积小、耗能低、寿命长等优点, 已广泛应用于通用照明和背光显示领域, 其应用场景也在进一步拓展[1-6]。目前获得白光 LED 的主流方案是蓝光 LED 激发黄色荧光粉(YAG:Ce), 且大部分采用传统的“环氧树脂/有机硅脂+荧光粉”方式进行封装。这些有机透明材料的热导率极低且高温下易老化[7], 限制了其在高功率照明领域的应用。解决上述问题的有效方法是改用荧光陶瓷、单晶、玻璃陶瓷等块体材料作为全无机荧光转换体[8-15]。作为一类新型荧光玻璃陶瓷, Phosphor-in-Glass(PiG)复合体可以兼具荧光粉的高量子效率和玻璃基体的优良物理化学稳定性和较高热导率[14-18]。相比于荧光单晶或陶瓷, PiG 的制造工艺更简单、成本更低。因此, PiG 在大功率白光 LED 或激光照明领域具有巨大的应用潜力。

基于 YAG:Ce 黄色荧光粉的白光 LED, 由于光谱中缺乏红光成分, 只能得到相关色温(Correlated color temperature, CCT)大于 5500 K 的冷白光[9,19-20]。CCT 小于 5500 K 的正白光或暖白光更加符合人们对照明光源的需求, 特别适合于家居照明。尽管添加红色荧光粉可以获得高显色性的暖白光, 但是目前氮化物/氟化物红色荧光粉的物理化学稳定性差, 不能应用于高功率照明领域[21-26]。另一种策略是通过晶格工程降低 Ce^{3+}的 5d 能级高度使其发射光谱红移[27-33], 例如 Gd^{3+}取代 Y^{3+}可以获得橙黄色荧光粉(Y,Gd)AG:Ce[30-32]。已有的研究工作均是关于(Y,Gd)AG:Ce 透明陶瓷或者单晶[12,30-32], 已经报道的平板型全无机荧光转换体会导致白光 LED 的出光角小、效率低以及“黄环”等发光不均匀现象[8,15,34-35]。将远程荧光结构从传统的平板改为半球、钟型和钹形等曲面立体结构不仅可以显著改善 LED 器件的角度颜色均匀性, 而且能提高器件的出光效率, 沿中心角具有较厚荧光粉层的几何形状可以更好地匹配蓝光 LED 芯片的朗伯发射[36-39]。但是, 传统粉末烧结和单晶生长均极难实现三维立体结构, 增材制造(3D 打印)作为一种快速成形技术, 具有高度的可定制性, 并已在无机材料的个性化和模块化生产方面展示出巨大潜力[14,40-41]。

本工作在前期研究的基础上[14], 选取非晶态纳米二氧化硅(SiO_2)和(Gd,Y)AG:Ce 橙黄色荧光粉为主要原料, 设计了一种可光固化复合浆料, 然后通过光固化成型、排脂和还原气氛烧结等步骤获得了一系列高效率的(Gd,Y)AG:Ce-PiG 荧光体, 并对其晶体结构、形貌、发光特性和 LED/LD 器件性能等进行详细表征和分析, 还探索了不同掺杂荧光粉浓度对 LED 器件的流明效率、显色指数(Color rendering index, CRI)和 CCT 等光学参数的影响。最后, 通过 DLP 3D 打印技术演示了本制造方法在实现三维立体远程荧光体上的可行性。

1 实验方法

1.1 实验原料

原料主要包含: 甲基丙烯酸羟乙酯(HEMA, 96%, 阿拉丁)、聚乙二醇二丙烯酸酯(PEGDA400, 阿拉丁)、二甘醇二苯甲酸酯(DEDB, 99.5%, 佛山今佳新材料)、2,2-二甲氧基-2-苯基苯乙酮(DMPA, 99%, 阿拉丁)、光引发剂 Irgacure819(德国 Basf)和苏丹红 G(95%, 阿拉丁)组成、气相二氧化硅(Aerosil OX50, 德国 Evonik)、(Gd,Y)AG:Ce 荧光粉(中心波长为 575 nm)。

1.2 (Gd,Y)AG-PiG 的制备

可光固化浆料的制备: 将体积分数 67%的 HEMA、3%的 PEGDA400 和 30%的 DEDB 混合均匀后加入平均粒径为 40 nm 的气相二氧化硅并充分搅拌, 其中溶液和气相二氧化硅的体积约比为 6∶4。然后, 在上述浆料中添加质量分数 0.26%的紫外光引发剂 DMPA(若用于 3D 打印则替换为 Irgacure819, 并额外加入质量分数 0.004%的苏丹红 G)。最后加入一定质量分数的橙色荧光粉(Gd,Y)AG:Ce, 并充分搅

拌和除泡。

光固化成型: 将所得浆料倒入特定形状的模具中, 放置在 1000 W 的 365 nm 紫外灯下照射 30 s 进行固化成型, 或者倒入 DLP 3D 打印机(MoonRay-S, 浙江迅实科技)料槽中进行前驱体的 3D 打印成型。

脱脂: 将成型后的前驱体放入高温箱式炉中, 缓慢加热到 600 ℃, 并保温 10 h。

烧结: 将上述多孔坯体放入高温管式炉中, 并通入弱还原气体($V(N_2)$: $V(H_2)$=95 : 5), 在 1250 ℃下烧结 3 h, 即得到完全致密化的(Gd,Y)AG-PiG 样品。

1.3　晶体结构与发光特性表征

采用紫外–可见分光光度计(U-4100, 日立)测量样品的透射光谱。样品的晶体结构由粉末 X 射线衍射(XRD)谱仪(D/MAX 2550/PC, Rigaku)确认, 由配有能量色散光谱仪(INCA Energy Coater, 牛津仪器)的扫描电子显微镜(SEM, Utral-55, 卡尔·蔡司)分析样品的微观形貌和元素分布。用光学显微镜(BX53M, 奥林巴斯)拍摄光学显微图, 使用激光扫描共聚焦显微镜(SP5, 徕卡)分析石英玻璃中荧光粉颗粒的分布情况。用 FLS920P 光谱仪(爱丁堡)获得发射和激发光谱, 其中在测试变温发射光谱时, 使用高温荧光测试装置(TAP02, 东方科捷)控制温度。使用紫外近红外绝对量子产率测量仪(Quantaurus-QY Plus C13534-12, 滨松)测量样品的内量子效率(Internal quantum efficiency, IQE)和吸收率(Absorption efficiency, AE)。

1.4　白光 LED/LD 器件的封装与测试

将制得的 PiG 圆片抛光至指定厚度, 并切割成 10 mm×10 mm 的正方形, 直接嵌入到高功率(10 W)蓝光 LED 芯片, 并用导热硅胶密封, 得到高功率白光 LED 器件。采用配有积分球(SPEKTRON R98, ϕ50 cm)的 LED 综合测试系统(LHS-1000, 杭州远方光电)测量 LED/LD 器件的光学性能, 如 CCT、CRI、流明效率和色坐标等。基于上述测试系统, 本课题组自行搭建了激光照明测试系统对蓝光激光激发下的光色度参数进行测试, 其中激发光源为功率可调的 450 nm 半导体激光器(Laser diodes, LD)(宁波远明光电, LSR450CP-15W)。

2　结果与讨论

2.1　晶体结构和形貌分析

如图 1(a)所示, 掺杂了(Gd,Y)AG:Ce 荧光粉的样品均能在蓝光激发下发射明亮的橙黄光。图 1(b)

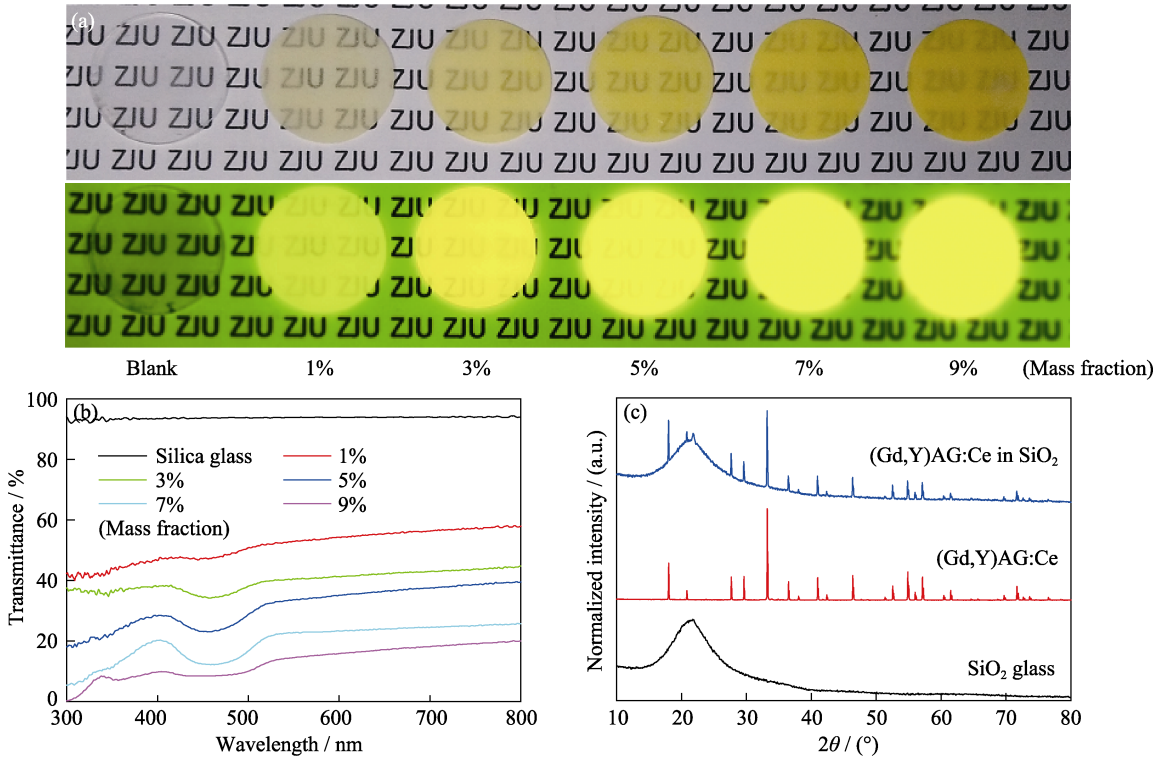

图 1　(Gd,Y)AG:Ce-PiG 的照片、透过率曲线和 XRD 图谱

Fig. 1　Photographs, transmittance spectra, and XRD patterns of (Gd,Y)AG:Ce-PiG

(a) (Gd,Y)AG:Ce-PiG (0.5 mm in thickness) with different doping concentrations under daylight and blue light (using a 480 nm filter to filter out blue light when taking pictures); (b) Transmittance spectra of (Gd,Y)AG:Ce-PiG samples; (c) XRD patterns of silica glass, (Gd,Y)AG:Ce phosphors and (Gd,Y)AG:Ce-PiG

Colorful figures are availuable on the website

为(Gd,Y)AG:Ce-PiG样品在300~800 nm的透过率曲线。随着(Gd,Y)AG:Ce 掺杂浓度的增加, 样品的全透过率逐渐降低。这是因为荧光粉颗粒(n≈1.85)和石英玻璃(n≈1.46)之间存在较大的折射率差异, 当荧光粉浓度增大时, 样品对入射光的散射作用增强, 透过率下降。此外, 添加荧光粉之后, 样品在 450 nm 处出现一个很强的吸收带, 这来源于(Gd,Y)AG:Ce 中 Ce^{3+}离子对蓝光的吸收。从样品的XRD 图谱(图 1(c))可知, (Gd,Y)AG:Ce 颗粒在致密化烧结后仍保留石榴石立方相, 从而形成一种荧光粉–玻璃复合体(PiG)。

如图 2(a~c)所示, 荧光粉均匀分布在石英玻璃的表面和内部, 没有出现明显的团聚现象。光固化成型所需时间极短(30 s), 有效避免了传统热固化成型中存在的荧光粉沉降现象。从 SEM 照片(图 2(d))可以看出, (Gd,Y)AG:Ce 颗粒与 SiO_2 玻璃的界面非常清晰, 表明二者在高温烧结时没有发生明显的反应。对样品进行元素能谱分析(EDS 面扫描), 如图 2(e, f)所示, Al 元素(代表(Gd,Y)AG:Ce 颗粒)存在的区域没有 Si 元素(代表 SiO_2 玻璃基质), 反之亦然。这些结果表明在高温烧结时(Gd,Y)AG:Ce 颗粒几乎没有受到石英玻璃的侵蚀, 即完好地嵌入到石英玻璃中, 使得 PiG 样品可以同时拥有荧光粉的发光性能和石英玻璃的物理化学稳定性。

2.2 (Gd,Y)AG:Ce-PiG 的发光性能

图 3(a)为(Gd,Y)AG:Ce-PiG 的激发和发射光谱。在 460 nm 蓝光激发下, PiG 发射峰值波长为 575 nm 的宽带橙黄光, 两个激发带位于在 340 和 460 nm 附近, 这些均源于(Gd,Y)AG:Ce 中 Ce^{3+}离子的 4f-5d 跃迁。相对于 YAG:Ce 黄色荧光粉(≈540 nm), (Gd,Y)AG:Ce 的发射峰明显红移, 主要是因为 Gd^{3+}取代 Y^{3+}导致 5d 能级的晶场劈裂增加, 5d 与 4f 之间的能量差变小[30]。如图 3(b)所示, (Gd,Y)AG:Ce-PiG 样品对蓝光(450 nm)的吸收率随着荧光粉掺杂浓度先增加后减小, 而内量子效率均在 90%左右, 其中, 质量分数 5%和 7%掺杂的 PiG 的 IQE 高达 91.2%。相比于(Gd,Y)AG:Ce 荧光粉(IQE=93.3%), (Gd,Y)AG:Ce-PiG 样品的内量子效率仅下降了 2%。进一步测试了(Gd,Y)AG:Ce-PiG 的变温荧光光谱(图 3(c))。随着温度升高, 发光强度单调下降, 这是因为在高温下激发态电子更容易被热激活到导带或者通过位形坐标的交叉点无辐射弛豫[12]。PiG 和荧光粉的积分发光强度随着温度的变化曲线几乎重合(图 3(d))。这些结果说明在还原气氛的保护下, 即使在 1250 ℃ (3 h)下(Gd,Y)AG:Ce-PiG 仍保留了相应荧光粉的发光性能, 也证明了(Gd,Y)AG:Ce 与石英玻璃之间非常有限的界面反应。

2.3 高功率 LED/LD 性能测试

为展示(Gd,Y)AG:Ce-PiG 在高功率领域的应用潜力, 使用(Gd,Y)AG:Ce-PiG 薄片与高功率(10 W) 460 nm LED 芯片组装成白光 LED 原型器件。图 4(a)为基于不同掺杂浓度 PiG 的 LED 器件及其电致发光光谱(100 mA)。表 1 列出了基于不同掺杂浓度 PiG 的 LED 器件的流明效率、CCT 和 CRI 等参数。

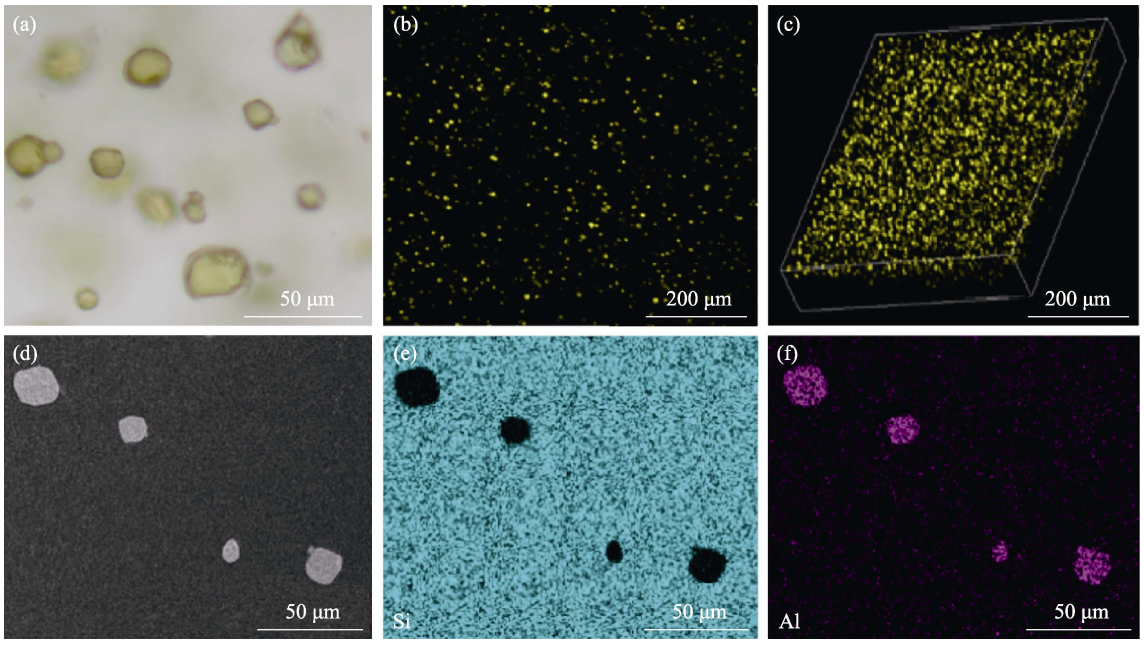

图 2 3%(质量分数)掺杂(Gd,Y)AG:Ce-PiG 的光学照片和能谱分析

Fig. 2 Optical photos and EDS images of 3% (mass fraction) (Gd,Y)AG:Ce-PiG

(a) Fluorescence microscope image; (b, c) 2D and 3D confocal laser scanning microscope images; (d) SEM image; (e, f) EDS spectra of Si and Al

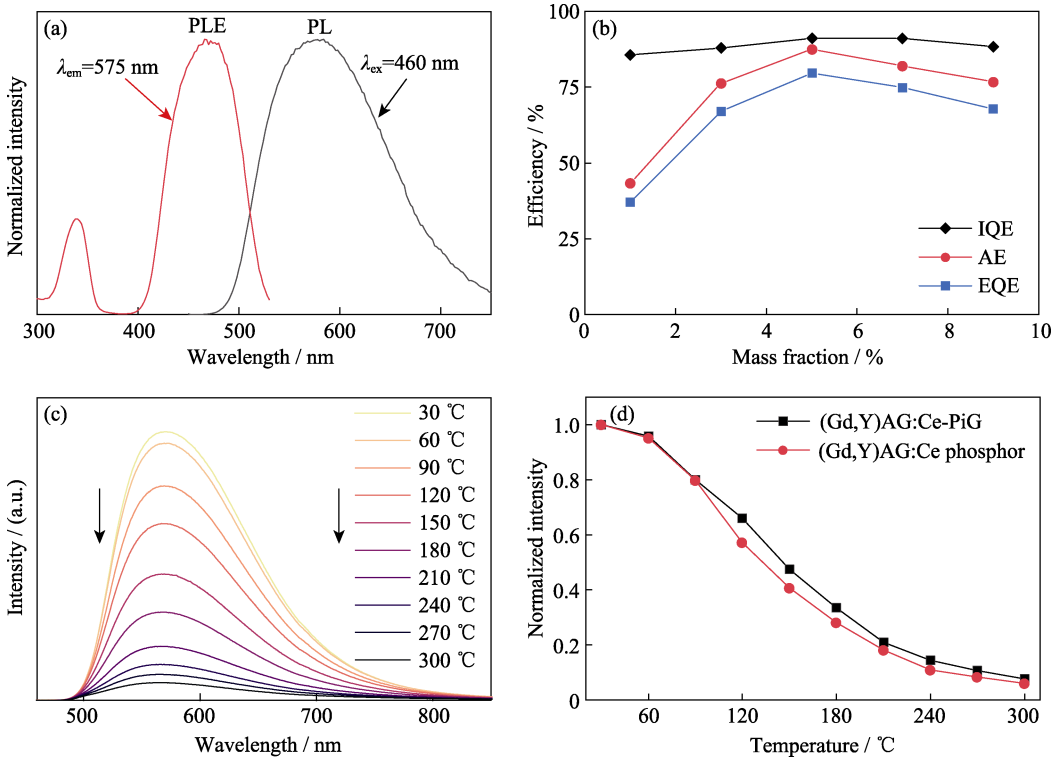

图 3　(Gd,Y)AG:Ce-PiG 的发光性能

Fig. 3　Luminous performance of (Gd,Y)AG:Ce-PiG

(a) Excitation and emission spectra of 5% (mass fraction) (Gd,Y)AG:Ce-PiG; (b) Values of internal quantum efficiency (IQE), absorption efficiency (AE) and external quantum efficiency (EQE) of (Gd,Y)AG:Ce-PiG with different doping concentrations; (c) Temperature-dependent emission spectrum of 5% (mass fraction) (Gd,Y)AG:Ce-PiG PiG; (d) Temperature dependences of integrated emission intensity of (Gd,Y)AG:Ce-PiG and (Gd,Y)AG:Ce phosphor

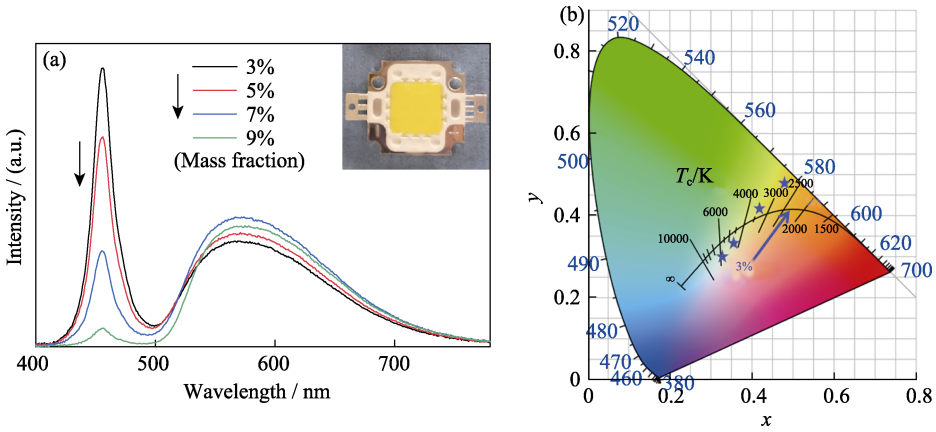

图 4　白光 LED 器件的电致发光光谱及其相应的 CIE 色坐标

Fig. 4　Electroluminescence spectra and their corresponding CIE color coordinates of white LEDs

(a) Electroluminescence spectra; (b) Corresponding CIE color coordinates. White LEDs fabricated by using (Gd,Y)AG:Ce-PiG (0.8 mm in thickness) with different doping concentrations under the current of 100 mA; The inset shows the picture of LED device

表 1　白光 LED 器件的光学性能

Table 1 Optical performance of the packaged white LED devices

Concentration (mass fraction)	Luminous efficiency/(lm·W^{-1})	CCT/K	CRI
3%	70.7	5717	84.1
5%	74.2	4444	78.4
7%	81.9	3398	67.7
9%	72.9	2907	60.5

相比于传统“蓝光 LED+黄色 YAG:Ce 荧光粉”白光 LED, 基于(Gd,Y)AG:Ce 的白光 LED, 其光谱中红光成分更多, 因此, 可以通过荧光粉浓度调节 LED 和荧光粉的光谱比例实现从冷白光到暖白光的调控(表 1 和图 4(b))。掺杂浓度为质量分数 5%的(Gd,Y)AG:Ce-PiG 制成的白光 LED 器件的流明效率可达 74.2 lm/W, CCT 为 4444 K, CRI 为 78.4, 而 YAG:Ce 仅能实现 CCT > 5500 K 冷白光输出[9,19-20]。使用如图 5(a)所示的反射式激光照明测试系统进一步探究了样品在高功率密度激发下的荧光转换能力。如图 5(b)所示, 掺杂浓度为质量分数 5%的(Gd,Y)AG:Ce-PiG 样品(厚度 0.8 mm)在蓝色激光辐照下的发射强度随激光功率的增加而增大, 在 2.84 W·mm^{-2} 下达到最大值, 此时 LD 照明器件的流明通量达到 180 lm。(Gd,Y)AG:Ce-PiG 的输出饱和阈值随着荧光粉掺杂浓度的增加而变小(图 5(c)), 这是因为 PiG 样品对激发光的吸收增强, 进而产生更多的热量, 最终因样品温度升高而导致(Gd,Y)AG:Ce 荧光猝灭[8, 24]。相应的 CCT、CRI 和辐射流明效率(Luminous efficiency of radiation, LER)如图 5(d)所示。CCT 和 CRI 在 PiG 未达到发光饱和时均变化较小, 而 LER 则呈单调下降趋势, 主要是因为在高功率激光激发下, PiG 的工作温度上升, Ce^{3+}的非辐射跃迁几率增加。这些结果表明(Gd,Y)AG:Ce-PiG 适合用作中高功率暖白光 LED/LD 的荧光转换材料。

2.4 3D 打印荧光转换体

目前基于“荧光粉+有机硅脂”以及荧光无机块体材料(如陶瓷、单晶以及 PiG)的高功率 LED 均采用平面型结构进行封装[8,15]。研究表明, 曲面立体结构的荧光转换体不仅能提高 LED 器件的出光效率, 还能改善其颜色均匀性[36-39]。采用一台桌面 DLP 3D 打印机演示了三种立体结构的 3D 打印制造, 分别为半球形、半球–圆柱型和半椭球形, 如图 6(a~c)。3D 打印的远程荧光体前驱体在烧结后能够保持原始形状, 表面亦无明显裂纹, 且内量子效率均在 90%左右。将得到的 PiG 直接覆盖在 1 W 的 460 nm LED 芯片上, 即可组装成相应的白光 LED(图 6(d))。考虑到目前 3D 打印 PiG 前驱体的成品率较低, 相关工艺还有待进一步优化。通过合理的光学设计和优化的 3D 打印和烧结工艺, 该方法将大幅改善高功率白光 LED 的光学性能。

3 结论

本研究基于非晶态纳米复合浆料的光固化成型

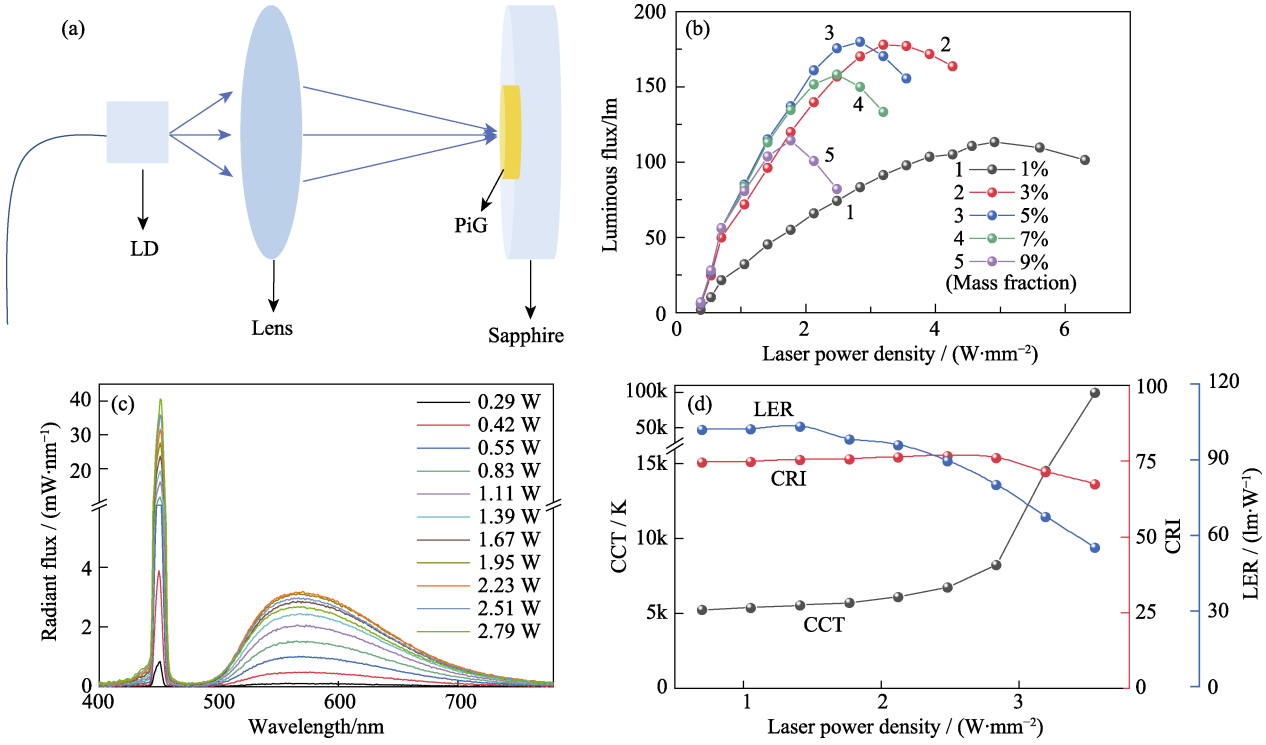

图 5 高功率下(Gd,Y)AG:Ce-PiG 的光学性能

Fig. 5 Optical performance of (Gd,Y) AG:Ce-PiG under high power

(a) Schematic of reflective LD device; (b) Luminous flux of (Gd,Y)AG:Ce-PiG (0.8 mm in thickness) with different doping concentrations as a function of the laser power density; (c) Emission spectra of 5% (mass fraction) (Gd,Y)AG:Ce-PiG under different laser powers densities; (d) Values of CCT, CRI and luminous efficacy of radiation (LER) of 5% (mass fraction) (Gd,Y)AG:Ce-PiG under different laser power densities
Colorful figures are availuable on the website

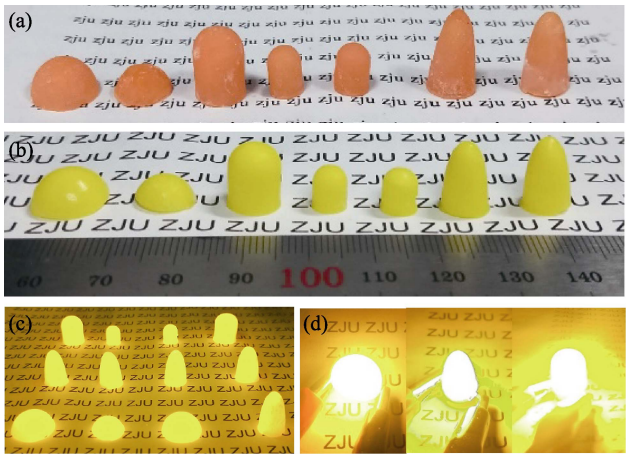

图 6　3D 打印荧光转换体

Fig. 6　3D printed fluorescence converter

(a) Photos of 5% (mass fraction) doped 3D printed precursor; (b) Photos of sintered (Gd,Y)AG:Ce-PiG; (c) Sintered (Gd,Y)AG:Ce-PiG under 450 nm blue light irradiation; (d) Device demonstration of white LED when combined with blue LED chip

和无压致密化烧结, 制备了一种与 3D 打印兼容的荧光玻璃陶瓷(PiG)复合材料。得益于石英玻璃和(Gd,Y)AG:Ce 荧光粉之间微弱的界面反应, 成功制备了一种橙黄色全无机荧光转换体, 其不仅内量子效率高(>90%)和热稳定性较好, 还能够实现曲面立体结构。利用(Gd,Y)AG:Ce-PiG 可以封装得到 CCT<4500 K、CRI>75 暖白光 LED, 且能够耐受 2.84 W·mm^{-2} 的蓝光激光密度辐照, 在中高功率暖白光固态光源领域展示出较大潜力。全无机荧光转换体的 3D 打印将推动高功率白光 LED 进入个性化和模块化阶段。

参考文献:

[1] PATTISON P M, TSAO J Y, BRAINARD G C, *et al.* LEDs for photons, physiology and food. *Nature*, 2018, **563(7732):** 493–500.

[2] CAO X, CAO C C, SUN G Y. Recent progress of single-phase white light-emitting diodes phosphors. *Journal of Inorganic Materials*, 2019, **34(11):** 1145–1155.

[3] ZHAO M, LIAO H, MOLOKEEV M S, *et al.* Emerging ultra-narrow-band cyan-emitting phosphor for white LEDs with enhanced color rendition. *Light: Science & Applications*, 2019, **8:** 38.

[4] BASORE E T, WU H, XIAO W, *et al.* High-power broadband NIR LEDs enabled by highly efficient blue-to-NIR conversion. *Advanced Optical Materials*, 2021, **9(7):** 2001660.

[5] ZHENG G, XIAO W, WU H, *et al.* Near-unity and zero-thermal-quenching far-red-emitting composite ceramics *via* pressureless glass crystallization. *Laser & Photonics Reviews*, 2021, **15(7):** 2100060.

[6] WEI Y, XING G, LIU K, *et al.* New strategy for designing orangish-red-emitting phosphor *via* oxygen-vacancy-induced electronic localization. *Light: Science & Applications*, 2019, **8:** 15.

[7] HUANG J, GOLUBOVIC D S, KOH S, *et al.* Rapid degradation of mid-power white-light LEDs in saturated moisture conditions. *IEEE Transactions on Device and Materials Reliability*, 2015, **15(4):** 478–485.

[8] LI S, WANG L, HIROSAKI N, *et al.* Color conversion materials for high-brightness laser-driven solid-state lighting. *Laser & Photonics Reviews*, 2018, **12(12):** 1800173.

[9] LI J, ZOU J, XIA C, *et al.* Ce:YAG transparent ceramics enabling high luminous efficacy for high-power LEDs/LDs. *Journal of Inorganic Materials*, 2021, **36(8):** 883–892.

[10] HU T, NING L, GAO Y, *et al.* Glass crystallization making red phosphor for high-power warm white lighting. *Light: Science & Applications*, 2021, **10(1):** 56.

[11] DING H, LIU Z, HU P, *et al.* High efficiency green-emitting LuAG:Ce ceramic phosphors for laser diode lighting. *Advanced Optical Materials*, 2021, **9(8):** 2002141.

[12] ARJOCA S, INOMATA D, MATSUSHITA Y, *et al.* Growth and optical properties of $(Y_{1-x}Gd_x)_3Al_5O_{12}$:Ce single crystal phosphors for high-brightness neutral white LEDs and LDs. *CrystEngComm*, 2016, **18(25):** 4799–4806.

[13] LIU X, HUANG Z, XIE R, *et al.* Phosphor ceramics for high-power solid-state lighting. *Journal of Inorganic Materials*, 2021, **36(8):** 807–819.

[14] ZHANG D, XIAO W, LIU C, *et al.* Highly efficient phosphor-glass composites by pressureless sintering. *Nature Communications*, 2020, **11(1):** 2805.

[15] LIN H, HU T, CHENG Y, *et al.* Glass ceramic phosphors: towards long-lifetime high-power white light-emitting-diode applications-a review. *Laser & Photonics Reviews*, 2018, **12(6):** 1700344.

[16] LEE Y K, LEE J S, HEO J, *et al.* Phosphor in glasses with Pb-free silicate glass powders as robust color-converting materials for white LED applications. *Optics Letters*, 2012, **37(15):** 3276–3278.

[17] YOU S, LI S, ZHENG P, *et al.* A thermally robust $La_3Si_6N_{11}$:Ce-in-glass film for high-brightness blue-laser-driven solid state lighting. *Laser & Photonics Reviews*, 2019, **13(2):** 1800216.

[18] ZHANG X, SI S, YU J, *et al.* Improving the luminous efficacy and resistance to blue laser irradiation of phosphor-in-glass based solid state laser lighting through employing dual-functional sapphire plate. *Journal of Materials Chemistry C*, 2019, **7(2):** 354–361.

[19] MA X, LI X, LI J, *et al.* Pressureless glass crystallization of transparent yttrium aluminum garnet-based nanoceramics. *Nature Communications*, 2018, **9(1):** 1175.

[20] SUN B, ZHANG L, ZHOU T, *et al.* Protected-annealing regulated defects to improve optical properties and luminescence performance of Ce:YAG transparent ceramics for white LEDs. *Journal of Materials Chemistry C*, 2019, **7(14):** 4057–4065.

[21] WANG L, XIE R J, LI Y, *et al.* $Ca_{1-x}Li_xAl_{1-x}Si_{1+x}N_3$:$Eu^{2+}$ solid solutions as broadband, color-tunable and thermally robust red phosphors for superior color rendition white light-emitting diodes. *Light: Science & Applications*, 2016, **5(10):** e16155.

[22] HOERDER G J, SEIBALD M, BAUMANN D, *et al.* $Sr[Li_2Al_2O_2N_2]$:Eu^{2+}-a high performance red phosphor to brighten the future. *Nature Communications*, 2019, **10(1):** 1824.

[23] RONGJUN X I E, DELIANG C, SETSUHISA T, *et al.* Advance in red-emitting Mn^{4+}-activated oxyfluoride phosphors. *Journal of Inorganic Materials*, 2020, **35(8):** 847–856.

[24] SENDEN T, VAN DIJK-MOES R J A, MEIJERINK A. Quenching of the red Mn^{4+} luminescence in Mn^{4+}-doped fluoride LED phosphors. *Light: Science & Applications*, 2018, **7:** 8–13.

[25] XU J, YANG Y, GUO Z, *et al.* Design of a $CaAlSiN_3$:Eu/glass composite film: facile synthesis, high saturation-threshold and application in high-power laser lighting. *Journal of the European Ceramic Society*, 2020, **40(13):** 4704–4708.

[26] DANG P, LI G, YUN X, *et al.* Thermally stable and highly efficient red-emitting Eu^{3+}-doped $Cs_3GdGe_3O_9$ phosphors for WLEDs:

non-concentration quenching and negative thermal expansion. *Light: Science & Applications*, 2021, **10(1):** 29.

[27] DU Q, FENG S, QIN H, *et al.* Massive red-shifting of Ce^{3+} emission by Mg^{2+} and Si^{4+} doping of YAG:Ce transparent ceramic phosphors. *Journal of Materials Chemistry C*, 2018, **6(45):** 12200–12205.

[28] SUN P, HU P, LIU Y, *et al.* Broadband emissions from $Lu_2Mg_2Al_2Si_2O_{12}:Ce^{3+}$ plate ceramic phosphors enable a high color-rendering index for laser-driven lighting. *Journal of Materials Chemistry C*, 2020, **8(4):** 1405–1412.

[29] LIU S, SUN P, LIU Y, *et al.* Warm white light with a high color-rendering index from a single $Gd_3Al_4GaO_{12}:Ce^{3+}$ transparent ceramic for high-power LEDs and LDs. *ACS Applied Materials & Interfaces*, 2019, **11(2):** 2130–2139.

[30] DIGONNET M J F, NISHIURA S, JIANG S, *et al.* Transparent Ce^{3+}:GdYAG Ceramic Phosphors for White LED. Proc. SPIE, Optical Components and Materials VIII, San Francisco, 2011**:** 793404.

[31] LIU X, QIAN X, HU Z, *et al.* Al_2O_3-Ce:GdYAG composite ceramic phosphors for high-power white light-emitting-diode applications. *Journal of the European Ceramic Society*, 2019, **39(6):** 2149–2154.

[32] CHEN J, TANG Y, YI X, *et al.* Fabrication of $(Tb,Gd)_3Al_5O_{12}:Ce^{3+}$ phosphor ceramics for warm white light-emitting diodes application. *Optical Materials Express*, 2019, **9(8):** 3333–3341.

[33] DING H, LIU Z, LIU Y, *et al.* $Gd_3Al_3Ga_2O_{12}$:Ce, Mg^{2+} transparent ceramic phosphors for high-power white LEDs/LDs. *Ceramics International*, 2021, **47(6):** 7918–7924.

[34] LIU Z, LIU S, WANG K, *et al.* Optical analysis of color distribution in white LEDs with various packaging methods. *IEEE Photonics Technology Letters*, 2008, **20(24):** 2027–2029.

[35] YU R, JIN S, CEN S, *et al.* Effect of the phosphor geometry on the luminous flux of phosphor-converted light-emitting diodes. *IEEE Photonics Technology Letters*, 2010, **22(23):** 1765–1767.

[36] LIU Z, KAI W, LUO X, *et al.* Realization of High Spatial Color Uniformity for White Light-emitting Diodes by Remote Hemispherical YAG: Ce Phosphor Film. Electronic Components and Technology Conference, Las Vegas, 2010**:** 1703–1707.

[37] TSAI P Y, HUANG H K, SUNG J M, *et al.* High thermal stability and wide angle of white light chip-on-board package using a remote phosphor structure. *IEEE Electron Device Letters*, 2015, **36(3):** 250–252.

[38] CHENG T, YU X, MA Y, *et al.* Angular color uniformity enhancement of white LEDs by lens wetting phosphor coating. *IEEE Photonics Technology Letters*, 2016, **28(14):** 1589–1592.

[39] LI J, LI Z, LI Z, *et al.* Improvement in optical performance and color uniformity by optimizing the remote phosphor caps geometry for chip-on-board light emitting diodes. *Solid-State Electronics*, 2016, **126:** 36–45.

[40] MOORE D G, BARBERA L, MASANIA K, *et al.* Three-dimensional printing of multicomponent glasses using phase-separating resins. *Nature Materials*, 2020, **19(2):** 212–217.

[41] CAMPOSEO A, PERSANO L, FARSARI M, *et al.* Additive manufacturing: applications and directions in photonics and optoelectronics. *Advanced Optical Materials*, 2019, **7(1):** 1800419.